Journal of Visualized Experiments

Manipulation of Single Neural Stem Cells and Neurons in Brain Slices Using Robotic Microinjection

--Manuscript Draft--

Article Type:	Methods Article - JoVE Produced Video
Manuscript Number:	JoVE61599R2
Full Title:	Manipulation of Single Neural Stem Cells and Neurons in Brain Slices Using Robotic Microinjection
Section/Category:	JoVE Bioengineering
Keywords:	brain development, stem cell, lineage tracing, robotics, neuron, microinjection, organotypic tissue slice, single cell manipulation
Corresponding Author:	Elena Taverna, Ph.D. Max-Planck-Institut Evolutionary Anthropologie Leipzig, Sachsen GERMANY
Corresponding Author's Institution:	Max-Planck-Institut Evolutionary Anthropologie
Corresponding Author E-Mail:	elena_taverna@eva.mpg.de
Order of Authors:	Gabriella Shull
	Christiane Haffner
	Elena Taverna, Ph.D.
	Suhasa Kodandaramaiah
Additional Information:	
Question	Response
Please indicate whether this article will be Standard Access or Open Access.	Open Access (US$4,200)
Please indicate the **city, state/province, and country** where this article will be **filmed**. Please do not use abbreviations.	Dresden, Germany

To the Journal of Visualized Experiments Editorial Board

We are pleased to submit the revised version of our work illustrating the use of the Autoinjector – a robotic platform for microinjection into single neural stem cells and neurons in brain tissue.

We hope we addressed all the issues raised by the Editor in a satisfactory manner.

Sincerely,

Suhasa Kodandaramaiah
Benjamin Mayhugh Assistant Professor
Department of Mechanical Engineering
The University of Minnesota, Twin Cities, USA

and

Elena Taverna
Department of Evolutionary Genetics,
Max Planck Institute for Evolutionary Anthropology, Leipzig, Germany

1 **TITLE:**
2 Manipulation of Single Neural Stem Cells and Neurons in Brain Slices Using Robotic
3 Microinjection
4
5 **AUTHORS AND AFIILIATIONS:**
6 Gabriella Shull[1,2*], Christiane Haffner[3*], Elena Taverna[3,4], Suhasa B. Kodandaramaiah[1,5,6]
7
8 [1]Department of Biomedical Engineering, University of Minnesota, Twin Cities
9 [2]Department of Biomedical Engineering, Duke University, Durham
10 [3]Max Planck Institute of Molecular Cell Biology and Genetics, Dresden, Germany
11 [4]Max Planck Institute for Evolutionary Anthropology, Leipzig, Germany
12 [5]Department of Mechanical Engineering, University of Minnesota, Twin Cities
13 [6]Graduate Program in Neuroscience, University of Minnesota, Twin Cities
14
15 [*] These authors contributed equally to this work.
16
17 Email Addresses of Corresponding Authors:
18 Elena Taverna   (elena_taverna@eva.mpg.de)
19 Suhasa Kodandaramaiah   (suhasabk@umn.edu)
20
21 Email Addresses of Co-Authors:
22 Gabriella Shull   (gabriella.shull@duke.edu)
23 Christiane Haffner   (haffner@mpi-cbg.de)
24

25 **KEYWORDS:**
26 brain development, stem cell, lineage tracing, robotics, neuron, microinjection, organotypic
27 tissue slice, single cell manipulation
28

29 **SUMMARY:**
30 This protocol demonstrates the use of a robotic platform for microinjection into single neural
31 stem cells and neurons in brain slices. This technique is versatile and offers a method of tracking
32 cells in tissue with high spatial resolution.
33
34 **ABSTRACT:**
35 A central question in developmental neurobiology is how neural stem and progenitor cells form
36 the brain. To answer this question, one needs to label, manipulate, and follow single cells in the
37 brain tissue with high resolution over time. This task is extremely challenging due to the
38 complexity of tissues in the brain. We have recently developed a robot, that guide a
39 microinjection needle into brain tissue upon utilizing images acquired from a microscope to
40 deliver femtoliter volumes of solution into single cells. The robotic operation increases resulting
41 an overall yield that is an order of magnitude greater than manual microinjection and allows for
42 precise labeling and flexible manipulation of single cells in living tissue. With this, one can
43 microinject hundreds of cells within a single organotypic slice. This article demonstrates the use
44 of the microinjection robot for automated microinjection of neural progenitor cells and neurons

45   in the brain tissue slices. More broadly, it can be used on any epithelial tissue featuring a surface
46   that can be reached by the pipette. Once set up, the microinjection robot can execute 15 or more
47   microinjections per minute. The microinjection robot because of its throughput and versality will
48   make microinjection a broadly straightforward high-performance cell manipulation technique to
49   be used in bioengineering, biotechnology, and biophysics for performing single-cell analyses in
50   organotypic brain slices.
51
52   **INTRODUCTION:**
53   This protocol describes the use of a robot to target and manipulate single cells in brain tissue
54   slices, focusing in particular on single neural stem cells and neurons. The robot was developed to
55   address a central question in developmental neurobiology, that is how neural stem and
56   progenitor cells contribute to the brain morphogenesis[1–5]. To answer this question, one needs to
57   label and track single neural stem cells and follow their lineage progression over time to correlate
58   single cell behavior with tissue morphogenesis. This can be achieved in different ways, e.g., by
59   electroporating brain tissue in utero or by labeling single cell using lipophilic dies. Although
60   powerful, these methods lack precise single cell resolution (electroporation) and/or the
61   possibility to manipulate the intracellular space (lipophilic dye). Microinjection into single cells
62   was developed to overcome this challenge[6–8]. During microinjection, a pipette is briefly inserted
63   into a single cell within intact tissue under pressure to microinject femtoliter volumes of
64   reagents[9]. We have previously described a manual procedure for microinjecting single neural
65   stem cells in organotypic tissue (**Figure 1A**)[10,11]. Microinjection into neural stem cells relies on the
66   use of a micropipette that is inserted into single neural stem cells to inject a solution containing
67   a fluorescent dye, along with other molecules of interest. The selective targeting of neural stem
68   cells is achieved by approaching the developing telencephalon via the ventricular surface (or
69   ventricle, see cartoon in **Figure 1A**), that is formed by the apical plasma membrane of apical
70   progenitors (cartoon in **Figure 1A**). This process must be repeated for each cell that the
71   experimenter desires to inject. Further, the success of microinjection is dependent on the precise
72   control of the depth and duration of micropipette injection in the tissue. Thus, despite the unique
73   advantages, manual microinjection is extremely tedious and requires considerable practice to
74   perform at reasonable throughput and yield, making this technique difficult to use in a scalable
75   fashion. To overcome this limitation, we have recently developed an image guided robot, the
76   Autoinjector[12] (or microinjection robot) that can automatically perform microinjections into
77   single cells.
78
79   The microinjection robot makes use of microscopic imaging and computer vision algorithms to
80   precisely target specific locations in 3-D space within tissue for microinjection (**Figure 1B**). The
81   microinjection robot can be constructed by making relatively simple modifications to an existing
82   microinjection setup. The overall schematic of the microinjection robot is shown in **Figure 1C**. A
83   pipette is mounted in a pipette holder attached to a three-axis manipulator. A microscope
84   camera is used to acquire images of the tissue and the microinjection needle. A custom pressure
85   regulation system is used to control the pressure inside the pipette and a programmable
86   micromanipulator is used to control the position of the microinjector pipette. The camera images
87   of the tissue and microinjection pipette are used to determine the spatial location of the
88   microinjection pipette tip and the locations at which microinjections need to be performed. The

software then calculates trajectories needed to move the pipette within the tissue. All the hardware is controlled by the software that we previously developed. All software is written in coding language (e.g., Python and Arduino) and can be download from https://github.com/bsbrl/Autoinjector with instructions. The graphical user interface (GUI) allows the user to image the tissue and micropipette, and to customize the trajectory of microinjection. Our system can be established using relatively simple modifications to an inverted microscope equipped with brightfield and epi-fluorescence filters.

First, we provide instructions on preparing brain organotypic tissue slices for microinjection. Then the protocol illustrates starting the microinjection robot followed by preparatory steps, such as pipette motion calibration, that need to be done prior to microinjection. This is followed by defining the injection parameters. After this, the user can define the trajectory used by the microinjection robot and start the injection procedure. The microinjected tissue (in this case brain organotypic tissue slices) can be kept in culture for different time periods depending on the experimental design[10,11]. The tissue can be processed to follow and study the identity and fate of the injected cells and their progeny. Alternatively, the microinjected cells can be followed using live imaging. Within the scope of this protocol, we demonstrate the use of the robot to automatically microinjection neural progenitor cells in organotypic slices of mouse E14.5 dorsal telencephalon. The robot is further capable of microinjection into newborns neurons in the mouse telencephalon, as well as in the human fetal telencephalon[12].

In summary, we describe a robotic platform that can be used to follow and manipulate single cells in tissue. The platform makes use of pressure and it is, therefore, extremely versatile as to the chemical nature of the compound to inject. In addition, it can be adapted to target cells other than stem cells. We expect our system to be easily adapted to other model systems as well.

PROTOCOL:

All animal studies were conducted in accordance with German animal welfare legislation, and the necessary licenses were obtained from the regional Ethical Commission for Animal Experimentation of Dresden, Germany (Tierversuchskommission, Landesdirektion Dresden). Organotypic slices were prepared from E14.5 or E16.5 C57BL/6 mouse embryonic telencephalon (Janvier Labs).

1.   Installation of software

1.1.   Follow instructions to install the software from https://github.com/bsbrl/Autoinjector.

2.   Preparation of reagents and pipettes

2.1.   Agarose: Prepare 3% agarose by separately dissolving 3 g of wide range agarose and 3 g low-melting point agarose in 100 mL of cell culture-grade PBS in two separate 200 mL glass bottles, respectively. Store at room temperature for up to 3 months.

132   2.2.   Tyrode solution: Dissolve 1 g of sodium bicarbonate and Tyrode's salt (use the content of
133   the entire bottle) and 13 mL of 1 M HEPES in 1 L of distilled water. Adjust the pH to 7.4. Filter the
134   solution through a 0.2 µm bottle-top filter.

135

136   2.3.   Slice culture medium (SCM): Add 10 mL of rat serum, 1 mL of 2 mM glutamine, 1 mL
137   penicillin-streptomycin (100x), 1 mL of N-2 supplement (100x), 2 mL of B27 supplement (50x) and
138   1 mL of HEPES (pH 7.3) buffer into 84 mL of Neurobasal medium. Aliquot 5 mL of SCM into 15 mL
139   tubes. Store at -20 °C.

140

141   2.4. CO_2-Independent Microinjection Medium (CIMM): Prepare 5x DMEM modified low-
142   glucose solution (without phenol red) by dissolving the powder in 200 mL of distilled water. Filter
143   solution through a 0.2 µm bottle-top filter (for the DMEM powder, use the content of the entire
144   bottle). To prepare 100 mL of CIMM, mix 20 mL of 5x DMEM modified solution, 1 mL of HEPES
145   buffer, 1 mL of N2 supplement (100x), 2 mL of B27 supplement (50x), 1 mL of penicillin-
146   streptomycin (100x), 1 mL of 2 mM glutamine and 74 mL of distilled water. Store the solution at
147   4 °C.

148

149   2.5.   Reconstitution buffer: Prepare the reconstitution buffer by dissolving 262 mM $NaHCO_3$,
150   0.05 N NaOH, 200 mM HEPES in distilled water. Sterilize the solution by filtration through a bottle-
151   top 0.22 µm filter system into a sterile glass bottle. Aliquot 500 µL of reconstitution buffer into
152   airtight microcentrifuge tubes. Store at 4 °C.

153

154   2.6.   Microinjection dye stock: Dissolve the fluorescently labeled Dextran in RNase free
155   distilled water (final concentration 10 µg/µL). Prepare 5 µL aliquots and store at -20 °C until use.

156

157   2.7.   Pull the microinjection pipettes from borosilicate glass capillaries (1.2 mm outer
158   diameter, 0.94 mm inner diameter) using the micropipette puller. Protect the pipettes from dust.
159   Do not store pipettes for more than 2 – 3 days. For this experiment, the pulling parameters were
160   HEAT: ramp temperature +1 – 5; PULL: 100; VEL: 110; DEL: 100. HEAT and VEL are the parameters
161   that affect the most shape and size of the pipette.

162

163   NOTE: The optimal microinjection pipette has a long and flexible tip, to avoid cell damage during
164   microinjection.

165

166   **3.**   **Tissue slice preparation**

167

168   3.1.   Melt the 3% wide range agarose using a microwave oven prior to the brain tissue
169   dissection. Do not let the agarose solidify by keeping in a water bath at 37 °C prior to embedding.
170   Ensure that the pipettes are protected from dust. Do not store pipettes for more than 2 – 3 days.

171

172   3.2.   Thaw an aliquot of SCM and warm 10 – 12 mL CIMM and 20 mL of Tyrode's solution to 37
173   °C using a water bath.

174

3.3.   Mix the fluorescent tracer (Dextran-3000 or Dextran-10000-Alexa conjugated; final concentration 5 – 10 µg/µL) with the other chemical(s) to be injected. Centrifuge the microinjection solution at 16, 000 x g for 30 min at 4 °C. Collect the supernatant and transfer into a new tube. Keep the microinjection solution on ice until use.

3.4.   Use the heads from E13.5 – E16.5 mouse embryos to prepare organotypic tissue slices of the telencephalon. Remove the skin and open the skull using the forceps, moving along the midline. Dissect out the embryonic brain from the open skull and remove the meninges covering the brain tissue starting from the ventral side of the brain. Leave the dissected whole brain in Tyrode's solution on a 37 °C heating block.

NOTE: All dissection steps described in 3.4 must be performed in prewarmed Tyrode's solution.

3.5.   Pour the wide range melted agarose into a disposable embedding mold. When the agarose is cooled to 38 – 39 °C, carefully transfer the brains (a maximum of 4) into it using a Pasteur pipette. Always use cut tips for this step.

3.6.   Stir the agarose around the tissue either using a spatula or a pair of Dumont #1 forceps without touching the tissue. Let the agarose solidify at room temperature. Once the agarose has solidified, trim the excess agarose surrounding the tissue.

3.7.   Fill the buffer tray with PBS. Orient the brain with the rostro-caudal axis of the tissue perpendicular to the tray (use as landmark the olfactory bulbs, representing the rostral-most part of the brain). Cut 250 µm slices using a vibratome.

3.8.   Fill a 3.5 cm Petri dish with 2 mL of prewarmed media. Using a plastic Pasteur pipette, transfer slices (10 - 15) to this dish. Once done, shift the Petri dish with the slices into the slice culture incubator. Maintain slices at 37 °C in a humidified atmosphere containing 40% O_2 / 5% CO_2 / 55% N_2 until use.

4.   Microinjection

4.1.   Turn on the computer, microscope, microscope camera, manipulators, pressure rig, and pressure sensor. Load the application by clicking the file "**launchapp.py**" in the main folder downloaded from GitHub and specify the device settings in the popup screen (see step 1.1 for install instructions).

4.2.   Create an outward pressure to prevent unwanted clogging before submerging the pipette into the solution. To apply pressure to the pipette, slide the **compensation pressure** bar to 24 – 45% and click **Set Values**. Next, tune the pressure to a sufficient pressure by turning the mechanical pressure valve knob to 1 – 2 PSI (69 – 138 mbar) as indicated by the pressure sensor.

4.3.   Transfer the slices to a 3.5 cm Petri dish containing 2 mL of pre-warmed CIMM. Place the slices to be microinjected in the centre of the Petri dish. Transfer the Petri dish to the preheated (37 °C) microinjection stage.

4.4.   Load the microinjection pipette with 1.4 –1.6 µL of microinjected solution (from step 3.3) using a long-tip plastic pipette. Insert the microinjection pipette onto the pipette holder.

4.5.   Using the lowest magnification on the microscope, bring the slice into focus and guide the micropipette to this field of view (FOV) so that it is focused on the same plane as the slice target. Switch the output of the microscope to the camera to see the FOV in the application.

4.6.   Click the magnification button in the top left of the interface to initiate device calibration. A window will prompt to select the magnification. Select the 10x magnification, or whatever magnification the lens is set to (e.g., 4x, 10x, 20x, 40x) and press **Ok**. The software assumes the internal objective lens is 10x (the most common objective lens magnification).

4.7.   Refocus the pipette tip using the micrometric wheel of the microscope and click the pipette tip with the cursor. Next, press the **step 1.1** button and press **OK** in the popup window. The pipette will move in the Y direction. Click the tip of the pipette and press the **step 1.2** button. Lastly, enter **45** into the **Pipette angle** box and press the **Set angle**.

4.8.   Enter desired parameters into the **Automated microinjection controls** panel. For microinjection into apical progenitors set the injection distance to 20 – 40 µm and depth to 10 – 15 µm. For microinjection into neurons set the injection distance 30 – 40 µm from the basal side, and depth to 10 – 30 µm depending upon what is being targeted. Always set speed to 100%. Click **Set values**.

NOTE: The approach distance is the distance the pipette pulls out of the tissue before moving to the next injection distance, depth is the depth into tissue the microinjection goes, spacing is the distance along the line between sequential injections, speed is the speed of the pipette in µm/s.

4.9.   Click the **Draw edge** button and drag the cursor along the desired trajectory in the popup window to define the trajectory of injection. For microinjecting progenitor stem cells, the ventral side of the telencephalon surface is targeted as shown in **Figure 2A**. Bring the pipette to the start of the line and click the tip of the pipette. Click **Run trajectory** to start microinjecting. Repeat this step for every plane of injection targeted (usually done for 3 – 4 planes with 40 – 75 injections per plane).

5.   **Tissue culture and tissue slice processing for immunofluorescence**

5.1.   Prepare the collagen mixture (1.5 mg/mL): To a tube add 1.25 mL of the matrix solution, 0.5 mL of distilled water, 0.5 mL of 5x DMEM-F12 solution and 0.25 mL of reconstitution buffer. Keep it on ice until use.

5.2.   Obtain the Petri dish containing the microinjected slices from the slice culture incubation
262   chamber and immerse the slices into the collagen mixture.

263

264   5.3.   Transfer the slices together with 200 – 300 µL of collagen mixture into a 14 mm well of a
265   35 mm glass-bottom dish. Ensure that the slices are covered in very less collagen. This set up
266   allows for the optimal conditions for nutrients and oxygen uptake.

267

268   5.4.   Orient the slices while ensuring that there is enough space between the slices using two
269   pairs of forceps. Incubate the Petri dish for 5 min at 37 °C using a heating block to allow for the
270   collagen to solidify. Consider this time as t = 0 of slice culture.

271

272   5.5.   Move the Petri dish back to the slice culture incubator for an additional 40 min. Then add
273   2 mL of the prewarmed SCM. Slices are kept in culture until the desired time point.

274

275   5.6.   Take the slices out of the slice culture incubator and aspirate the SCM. Wash the collagen-
276   embedded slices with 1x PBS. Add 4% (wt/vol) paraformaldehyde (in 120 mM phosphate buffer,
277   pH 7.4) and leave the tissue at RT for 30 min. Then move it to 4 °C to allow for overnight fixation.

278

279   5.7.   Aspirate the paraformaldehyde solution the next day and perform 1x PBS washes. To
280   remove the slices from the collagen, use two pairs of forceps to gently extract the slices under a
281   stereomicroscope.

282

283   5.8.   Use a microwave to melt the 3% (wt/vol) low melting point agarose for processing the
284   microinjected slices. Pour the melted agarose into a disposable embedding mold and let it cool
285   to around 38 – 39 °C.

286

287   5.9.   Transfer the tissue slices from step 5.7 into this mold containing low melting agarose using
288   a plastic Pasteur pipette. Ensure that the pial side of the slice is up and the ventricular surface
289   faces down. If needed orient accordingly. Let the agarose cool down to RT to solidify.

290

291   5.10.   Trim the extra agarose surrounding the slices. Orient the agarose block to ensure that the
292   cut surface is parallel to the vibratome's cutting blade. Using vibratome, cut 50 µm thick sections.

293

294   5.11.   Fill a 24 well dish with 1x PBS. Transfer the sections into this dish using a fine-tip
295   paintbrush. Perform immunofluorescence as per the standard protocols.

296

297   **REPRESENTATIVE RESULTS:**
298   Microinjection serves the purpose of tracking and manipulating single neural stem cells and their
299   progeny in living tissue and to follow their lineage progression in a physiological environment. In
300   this article, we have demonstrated the use of the microinjection robot for targeting and
301   automatically microinjecting organotypic slices of the mouse telecephalon. **Figure 2** illustrates
302   representative images of successfully injected progenitor cells and **Figure 3** illustrates injected
303   newborn neurons. When injected with Dextran Alexa-488 (or Alexa-A555) dye, cells appear fully
304   filled with the dye. As for apical progenitors (**Figure 2**) confocal imaging allows reconstructing

305   with high spatial resolution the cell morphology, the presence -or absence- of the apical and basal
306   attachment, and to combine the morphological enquiry with marker expression. By combining
307   these criteria, the user can assign a specific cell fate to the microinjected cells and their progeny.
308   As for the neuron injection, the user can reconstruct the neuronal morphology, including the
309   structure and features of apical dendrite and axon. Automated microinjection can provide
310   significantly higher throughput as compared to manual microinjection (**Figure 2B**). Further, EdU
311   labeling confirms that cell viability is not affected by automation (**Figure 2C**). Keeping the
312   organotypic slice in culture allows following lineage progression of the microinjected cells (we
313   shown 4 - 24h in **Figure 2D**). If the microinjection solution contains genetic material (DNA, mRNA,
314   CRISPR-Cas9 guides) or recombinant proteins, then this allows studying if and how lineage
315   progression is affected by the manipulation.
316
317   Microinjection into single neural stem cells in tissue provides excellent single cell resolution and
318   for that reason it has been used to dissect the cell biology of neural stem cell progression and
319   fate transition (**Figure 3A**). Microinjection allows the delivery of complex mixture of chemicals.
320   We previously made use of this feature to study junctional coupling in neural progenitor cells by
321   mixing gap-junctional permeable with gap junctional impermeable fluorescent dyes[12]. We
322   extended previous work by studying junctional coupling in newborn neurons, by injecting Lucifer
323   Yellow along with Dextran-A555 (**Figure 3B**). As shown in **Figure 3B**, a proportion of newborn
324   pyramidal neurons are coupled via gap junctions to neighboring neurons. This observation is
325   consistent with the idea that immature neurons communicate via gap-junction[13,14]. Furthermore,
326   targeting neurons shows that the use of the microinjection robot can be generalized to several
327   cell types in the developing mammalian brain. This experimental setup will be useful to dissect
328   the cell biology of neurons in tissue, for example by delivering specific oligopeptides to interfere
329   with protein-protein interactions.
330
331   **TABLES AND FIGURES:**
332   **Figure 1: Automated microinjection setup and protocol.** (**A**) Overall protocol for tissue
333   preparation and automated microinjections using the microinjection robot. Right inset: Cartoon
334   schematic of mouse Telencephalon targeted for microinjection in this protocol. (**B**) Flowchart of
335   the automated microinjection steps. (**C**) Schematic of the microinjection robot hardware. (**D**)
336   Graphic user interface (GUI) of the software used to control and operate the microinjection
337   robot. This figure is adapted from ref. [12].
338
339   **Figure 2: Robotic microinjection into apical progenitors.** Schematic and expected results when
340   using the microinjection robot to target apical progenitors (APs) via the apical surface (apical
341   injection). (**A**) Top row. On the left: schematic of the process. On the right: GUI with relevant
342   parameters for apical injection. Bottom row. On the left: phase contrast image taken during the
343   injection procedure (V: ventricle; BL: basal lamina). On the right: representative results showing
344   microinjected APs. Dashed line represents the ventricle (V). Scale bar: 10 μm. (**B**) Successful
345   injections per minute for a novice user on the manual microinjection system, an experienced user
346   on the manual microinjection system, and the microinjection robot. (**C**) EdU incorporation in
347   microinjected cells and in non-injected cells in the injected area. Organotypic slices of mouse
348   E14.5 dorsal telencephalon were either (i) non injected or (ii) subjected to manual or automated

349   microinjection (injected slice) using Dextran-A488 (for manual and autoinjector). Slices were kept
350   in culture in the presence of EdU for 24 h, then they were fixed and stained for DAPI and EdU.
351   Injected and non-injected cells in the injected area were scored for EdU positivity. (**D**) Use of the
352   microinjection robot Lineage tracing. A fluorescent dye (Dx3-A555, magenta) is injected into
353   single neural stem cell (t = 0 h). The fluorescent dye is partitioned to the daughter cells (d1, d2)
354   during mitosis. This allows following the progeny of the injected cell (t = 4 h and 24 h) and
355   revealing the lineage progression over time. For t = 24 h, we show several examples of the
356   progeny one expects to find. Scale bars: 10 μm. Graphs in B and C are taken from ref.[12]
357
358   **Figure 3: Robotic microinjection into neurons.** Schematic and expected results when using the
359   microinjection robot to target pyramidal neurons (N) via the basal surface (basal injection). (**A**)
360   Top row. On the left: schematic of the process. On the right: GUI with relevant parameters for
361   basal injection. Bottom row. On the left: phase contrast image taken during the injection
362   procedure (V: ventricle; BL: basal lamina). On the right: representative results showing a
363   microinjected N. Dashed line represents the basal lamina (BL). Scale bar: 10 μm. (**B**) Use of the
364   autoinjector to study gap junctional communication in tissue. Pyramidal neurons were injected
365   with a solution containing two dyes: the gap junctional-impermeable Dx-A555 (not shown) and
366   the gap-junctional permeable Lucifer Yellow (green). Dx-A555 is confined to the targeted cell
367   (asterisks), while the LY diffuses to cells that are connected via gap junction to the targeted cell
368   (dashed lines). Left panel: Low exposure, only the microinjected cells are visible. Right panel: High
369   exposure allows visualization of the injected cells as well as the coupled cells (dashed lines). Scale
370   bar: 10 μm.
371
372   **Supplementary File: Troubleshooting several common errors that arise during microinjection.**
373
374   **DISCUSSION:**
375   Microinjection into single neural stem cells in tissue provides excellent single cell resolution and
376   for that reason it has been used to dissect the cell biology of neural stem cell progression and
377   fate transition (**Figure 2**; see also[10–12]). The automated microinjection procedure can be
378   performed on other types of cells in both embryonic mice and human brain tissue.
379   Representative results of microinjection of newborn neurons by targeting the basal surface of
380   the telencephalon are shown in **Figure 3**.
381
382   The principle established here can be applied to target several different cell types in embryonic
383   mouse brains and human brains. We have previously shown that the microinjection robot can
384   also be used to target single progenitor cells in the mouse hindbrain and telencephalon and
385   newborn neurons in the mouse and human developing neocortex[12]. To obtain the best results of
386   the injection procedure, one should optimize all the steps before starting the injection. It is
387   important to carefully consider and optimize the preparation of viable and well preserved
388   organotypic tissue slices from brain tissue (**Figure 1**). It is crucial to be quick in the dissection and
389   slicing procedure illustrated in **Figure 1**. For apical injection targeting the APs, one should pick
390   the slices showing the ideal orientation of the apical surface. For APs injection, the ideal
391   orientation is the apical surface perpendicular to the bottom of the Petri dish. Any other
392   orientation will be permissive as well, however, the apical surface perpendicular to the Petri dish

393 provides a wider surface area for injection, thus increasing the success of injection. For injection
394 into neurons, the orientation of the slice plays little to no effect.
395
396 Once the slices to inject are selected, the injection procedure per slice takes approximately 5
397 minutes. Considering that one works with living tissue, it is highly recommended to speed up the
398 injection procedure. To this end we recommend setting all the parameters for injection via the
399 GUI (**Figure 1D**) before the tissue is ready, to reduce any unnecessary waiting time. For
400 troubleshooting please refer to the **Supplementary file.**
401
402 In case of long-term slice culture, steps after the automated microinjection procedure can affect
403 the health of the cells and thereby the experiment. Therefore, it is highly recommended to run a
404 quality control test and to optimize the slice culture conditions. To evaluate cell viability after the
405 slicing and injection procedure, we performed EdU labeling during the culture and we quantified
406 the number of pyknotic nuclei (a proxy for apoptotic cells) in the cultures and injected tissue[12].
407 These quantifications did not reveal any significant impact of microinjection on tissue viability
408 (**Figure 2C**). We recommend running similar quality controls while establishing the organotypic
409 tissue slicing and microinjection pipeline in the lab.
410
411 Compared to manual microinjection, the microinjection robot provides several advantages. First,
412 the learning curve for the user is less steep as compared to manual injection: a new user will
413 reach a high proficiency after a limited number of sessions, typically 1 or 2. Second, in the case
414 of manual microinjection, a comparable proficiency requires months of training. The injection
415 procedure is faster and more efficient (**Figure 2B**). We quantified these parameters and found
416 that the microinjection robot outperformed a skilled manual user with respect to the injection
417 success (% of successful injection/total number of injections) and in the total number of injections
418 per unit time[12]. This results in an overall 300% increase of injection efficiency (% of successful
419 injection/min) for the microinjection robot compared to a skilled user. The increase in efficiency
420 was even more pronounced when comparing the microinjection robot with a beginner user and
421 reached 700%. Last but not the least, the microinjection robot can be easily programmed to
422 systematically explore all spatial parameters. This is particularly advantageous when adapting
423 the microinjection robot to target new cells or tissues, or when using the microinjection robot
424 for purposes requiring different spatial resolution.
425
426 Building the microinjection robot requires minimal changes to an existing epi-fluorescence
427 microscope[12]. We have previously provided instructions for this adaptation at
428 https://github.com/bsbrl/Autoinjector. Once the hardware is setup, this protocol provides key
429 methodological details for successfully undertaking automated microinjections. Overall, the
430 microinjection robot has a successful injection rate of 15.52 + 2.48 injections/min, which is 15x
431 greater than an inexperienced user (1.09 $\pm$ 0.67 injections/min), and 3x greater than an expert
432 user (4.95 $\pm$ 1.05 injections/min)[12]. This improvement in successful injection rate empowers both
433 novice and expert users to inject more cells in a shorter amount of time which is essential to
434 preserve tissue viability. Additionally, the microinjection robot is customizable and the trajectory,
435 depth of the injection, number of injections, spacing between injections can all be tuned using
436 the GUI. These features allow the microinjection robot to be used as a tool to optimize previously

437 laborious experiments, and to explore fundamentally new experiments that require higher yield
438 than previously possible.

439

440 The main limitations of the microinjection procedure we described here are related to the
441 preparation of tissue slices, a crucial step that needs extensive optimization. In addition,
442 microinjection relies on the presence of a surface that can be approached by the glass pipette.
443 This feature limits the type of tissues and tissue locations that can be targeted via microinjection
444 using the present setup.

445

446 The microinjection robot currently uses brightfield imaging and has been used in in vitro brain
447 slice preparations. In the future, the microinjection robot could be combined with 2-photon
448 imaging to increase the specificity of single cell targeting *in vivo* for molecular or dye tagging.
449 Such efforts have already been made for single cell electrophysiology[15,16]. The current device
450 requires manual observation of the microinjection procedure. Future versions could include
451 strategies for cleaning clogged microinjection pipettes[17] or integration of fluid handling robots[18]
452 for multiplexed, fully autonomous microinjections. These devices could increase the scale of
453 microinjection by orders of magnitude. Adapting algorithms for parallel control of multiple
454 microinjection pipettes[19] could enable multiplexed delivery of dozens of dyes and molecular
455 reagents into the same cells within the same experiments. This has the potential to open new
456 avenues for molecular screening in tissue.

457

458 The microinjection robot could be used to tag functionally identified cells using DNA or RNA
459 barcodes. This could in turn be combined with other single cell analysis techniques, such as single
460 cell RNA sequencing (scRNAseq) and electron microscopy. Our preliminary results show that
461 microinjected cells and their progeny can be recovered and isolated using tissue dissociation
462 followed by FACS sorting (Taverna, unpublished results). The FACS sorted cells can then be used
463 for scRNAseq. Furthermore, preliminary results show that the single cell resolution capabilities
464 of the microinjection robot can be used in combination with electron microscopic analysis to
465 explore the cell biology on neural stem cells in tissue at high spatial resolution (Taverna and
466 Wilsch-Bräuninger, unpublished results). These data suggest that the microinjection robot can be
467 used as a tool for correlative light and electron microscopy in tissue and in broader sense, for the
468 multimodal analysis of cell identity and behavior in tissue.

469

470 Microinjection relies on the use of pressure and one can afford injecting solutions with high
471 molecular complexity (e.g., an entire transcriptome). This feature of microinjection has been
472 exploited in the past for isolating and cloning ligand-gated receptors[20]. Along this line, the
473 microinjection robot might be used for modeling and studying multi-genic traits at the cellular
474 level. Combined with a sub-pooling strategy, the microinjection robot might also be used as a
475 platform to identify the minimum set of genes driving a certain trait/cellular behavior. Thus far,
476 the microinjection robot has been used to manipulate the cell's biochemistry via the delivery of
477 mRNA, DNA or recombinant proteins[10,21,22]. We foresee an application of the microinjection
478 robot in probing the biophysics of the intracellular space, for example, by delivering
479 nanomaterials or nanomachines that allow sensing and/or manipulation of the biophysical
480 properties of the intracellular space.

490 **DISCLOSURES:**
491 The authors have nothing to disclose.
492

493 **REFERENCES:**
494

495 1.   Taverna, E., Götz, M., Huttner, W. B. The Cell Biology of Neurogenesis: Toward an
496 Understanding of the Development and Evolution of the Neocortex. *Annual Review of Cell and*
497 *Developmental Biology*. **30** (1), 465–502 (2014).
498 2.   Götz, M., Huttner, W. B. The cell biology of neurogenesis. *Nature Reviews Molecular Cell*
499 *Biology*. **6** (10), 777–788 (2005).
500 3.   Di Lullo, E., Kriegstein, A. R. The use of brain organoids to investigate neural development
501 and disease. *Nature Reviews Neuroscience*. **18** (10), 573–584 (2017).
502 4.   Lancaster, M. A., Knoblich, J. A. Organogenesisin a dish: Modeling development and
503 disease using organoid technologies. *Science*. **345** (6194), 1247125 (2014).
504 5.   Kretzschmar, K., Clevers, H. Organoids: Modeling Development and the Stem Cell Niche
505 in a Dish. *Developmental Cell*. **38** (6), 590–600 (2016).
506 6.   Pepperkok, R. et al. Automatic microinjection system facilitates detection of growth
507 inhibitory mRNA. *Proceedings of the National Academy of Sciences of the United States of*
508 *America*. **85** (18), 6748–6752 (1988).
509 7.   Pepperkok, R., Lowe, M., Burke, B., Kreis, T. E. Three distinct steps in transport of vesicular
510 stomatitis virus glycoprotein from the ER to the cell surface in vivo with differential sensitivities
511 to GTPγS. *Journal of Cell Science*. **111** (13), 1877–1888 (1998).
512 8.   Pepperkok, R. et al. β-COP is essential for biosynthetic membrane transport from the
513 endoplasmic reticulum to the Golgi complex in vivo. *Cell*. **74** (1), 71–82 (1993).
514 9.   Ansorge, W., Pepperkok, R. Performance of an automated system for capillary
515 microinjection into living cells. *Journal of Biochemical and Biophysical Methods*. **16** (4), 283–292
516 (1988).
517 10.   Taverna, E., Haffner, C., Pepperkok, R., Huttner, W. B. A new approach to manipulate the
518 fate of single neural stem cells in tissue. *Nature Neuroscience*. **15** (2), 329–337 (2012).
519 11.   Wong, F. K., Haffner, C., Huttner, W. B., Taverna, E. Microinjection of membrane-
520 impermeable molecules into single neural stem cells in brain tissue. *Nature Protocols*. **9** (5),
521 1170–1182 (2014).
522 12.   Shull, G., Haffner, C., Huttner, W. B., Kodandaramaiah, S. B., Taverna, E. Robotic platform
523 for microinjection into single cells in brain tissue. *EMBO Reports*. **20** (10), e47880 (2019).
524 13.   Jabeen, S., Thirumalai, V. The interplay between electrical and chemical synaptogenesis.

525 *Journal of Neurophysiology*. **120** (4), 1914–1922 (2018).

526 14.   Nagy, J. I., Pereda, A. E., Rash, J. E. Electrical synapses in mammalian CNS: Past eras,
527 present focus and future directions. *Biochimica et Biophysica Acta - Biomembranes*. **1860** (1),
528 102–123 (2018).

529 15.   Suk, H.-J. et al. Closed-loop real-time imaging enables fully automated cell-targeted
530 patch-clamp neural recording in vivo. *Neuron*. **95** (5), 1037-1047 (2017).

531 16.   Annecchino, L. A. et al. Robotic automation of in vivo two-photon targeted whole-cell
532 patch-clamp electrophysiology. *Neuron*. **95** (5), 1048-1055 (2017).

533 17.   Kolb, I. et al. Cleaning patch-clamp pipettes for immediate reuse. *Scientific Reports*. **6**,
534 35001 (2016).

535 18.   Holst, G. L. et al. Autonomous patch-clamp robot for functional characterization of
536 neurons in vivo: development and application to mouse visual cortex. *Journal of*
537 *Neurophysiology*. **121** (6), 2341–2357 (2019).

538 19.   Kodandaramaiah, S. B. et al. Multi-neuron intracellular recording 1 in vivo via interacting
539 autopatching 2 robots. *ELife*. **7**, 24656 (2018).

540 20.   Lubbert, H. et al. cDNA cloning of a serotonin 5-HT1c receptor by electrophysiological
541 assays of mRNA-injected Xenopus oocytes (RNA fractionation/hybrid depletion/hybrid
542 selection/choroid plexus/voltage clamp). *Neurobiology*. **84** (2) 4332-4336 (1987).

543 21.   Florio, M. et al. Human-specific gene ARHGAP11B promotes basal progenitor
544 amplification and neocortex expansion. *Science*. **347** (6229), 1465–1470 (2015).

545 22.   Kalebic, N. et al. CRISPR/Cas9-induced disruption of gene expression in mouse embryonic
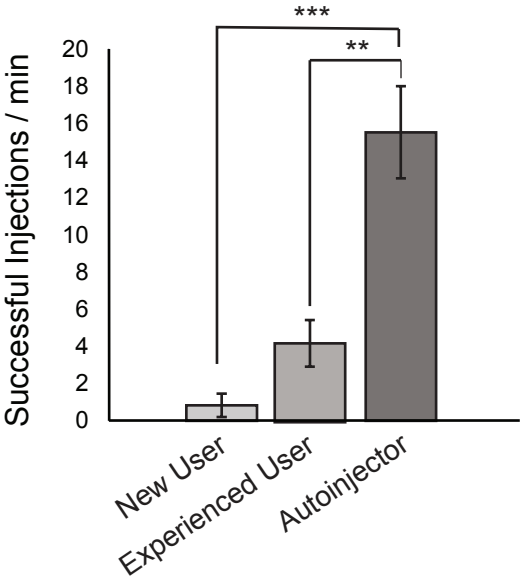546 brain and single neural stem cells in vivo. *EMBO Reports*. **17** (3), 338–348 (2016).
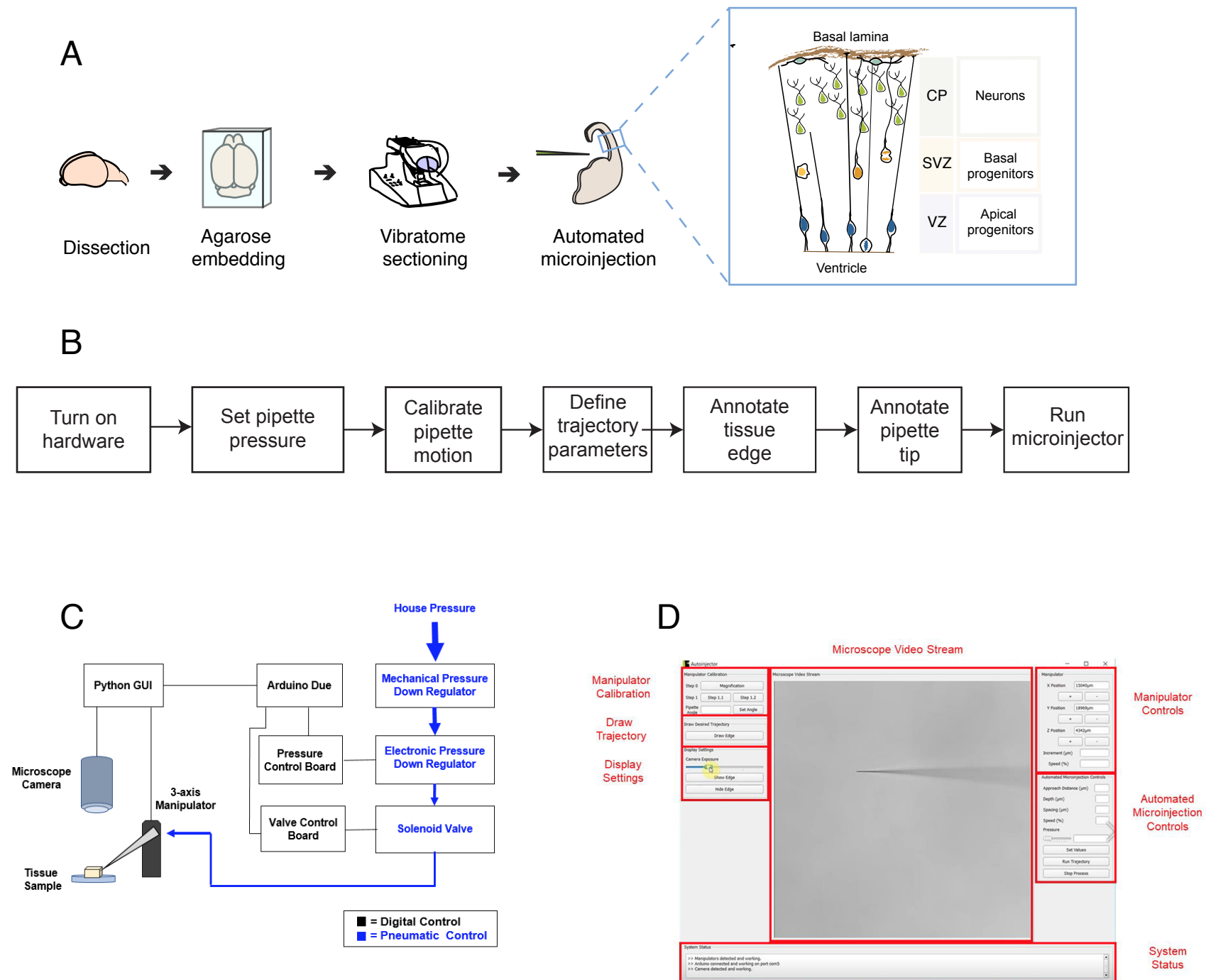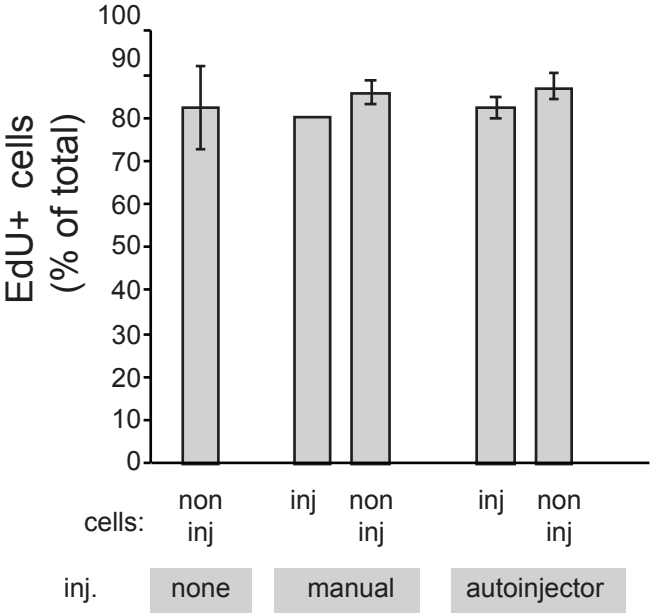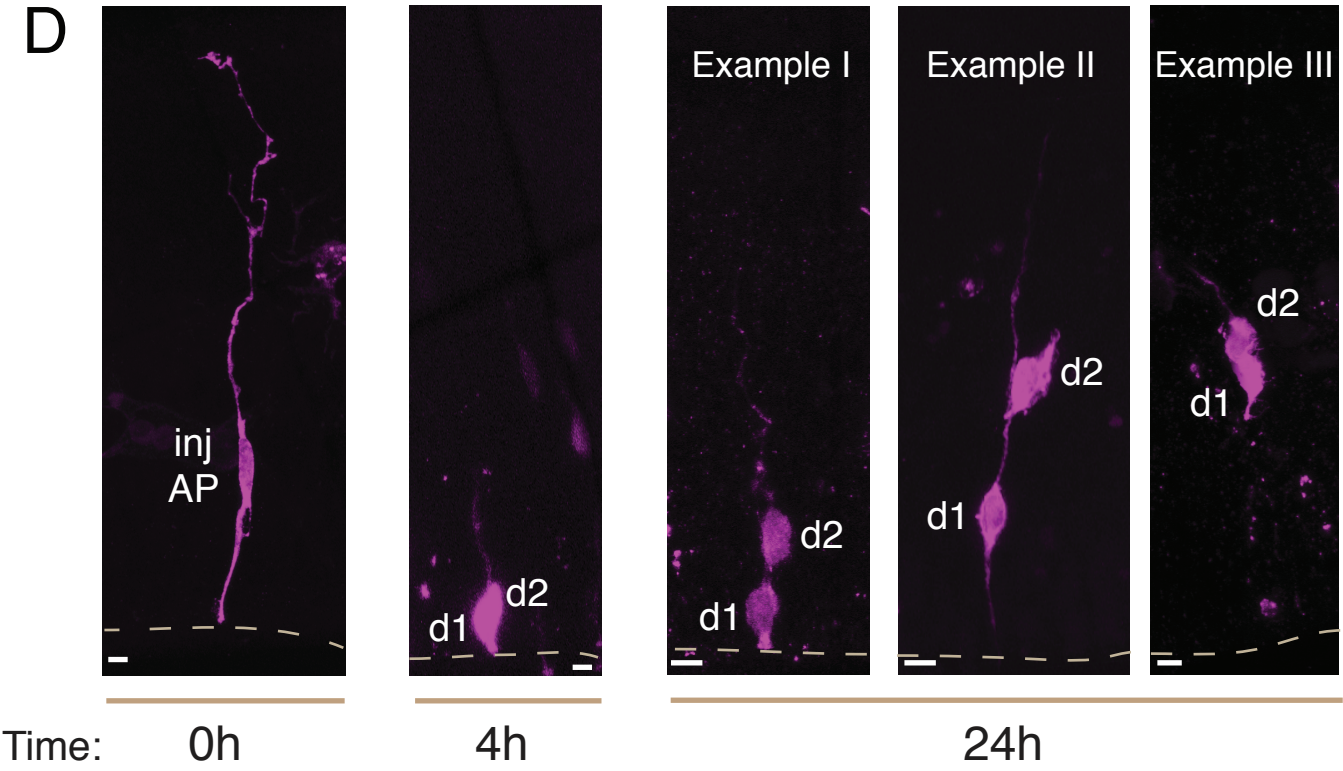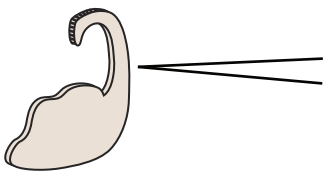
547
548

Figure 1

Shull et al. Figure 1
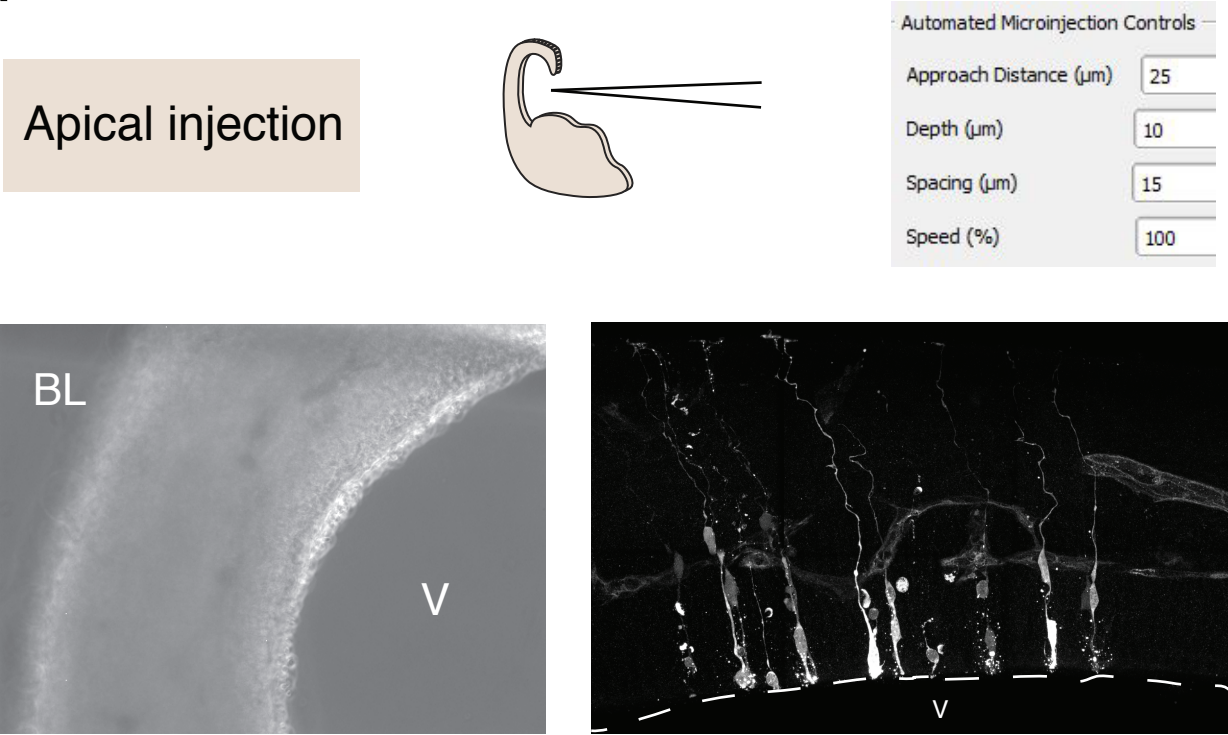
Figure 2

Figure 2. Shull et al.
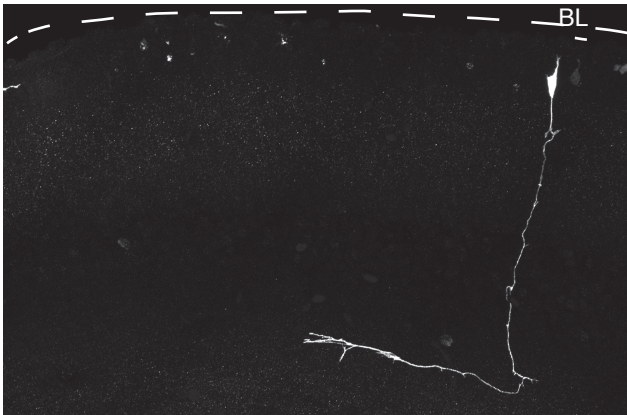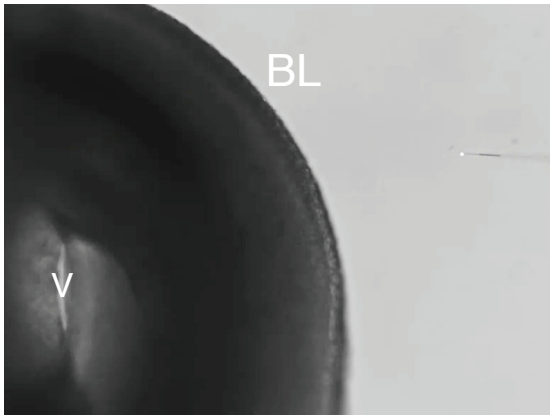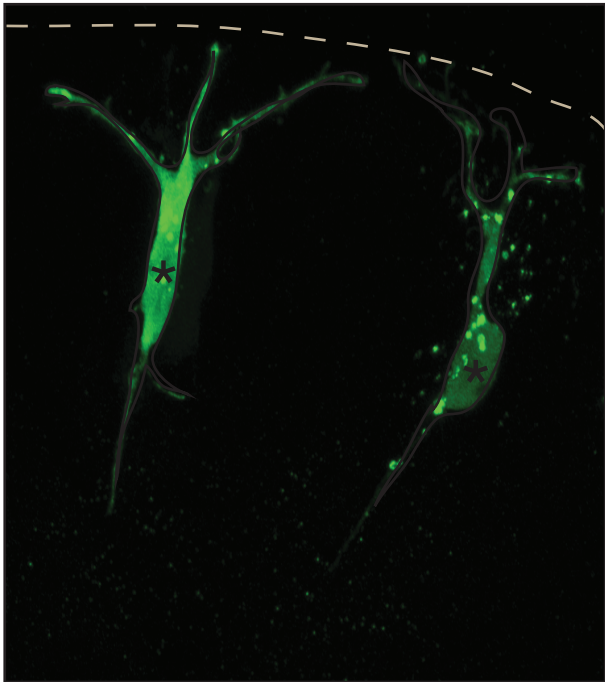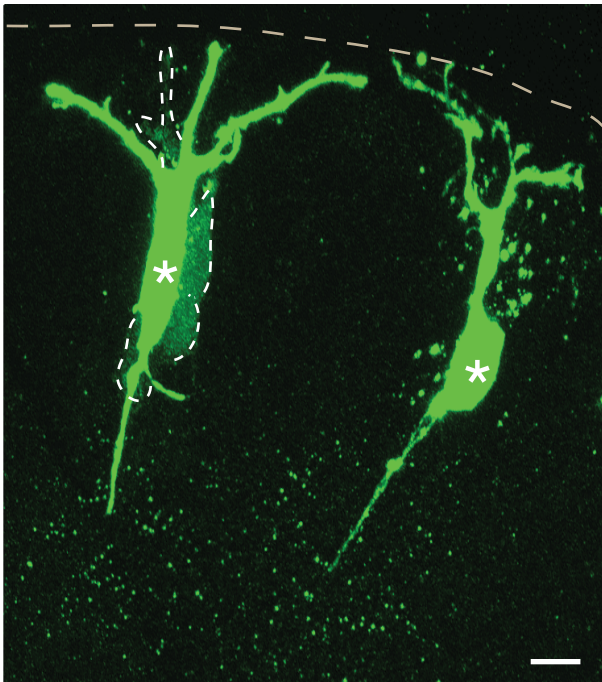
Figure 3

Confocal

Confocal_higher exposure

Figure 3. Shull et al.

Chemicals

Agarose, Low Melt	Ca
Agarose, Wild Range	Sig
Best-CA 221 Glue	Be
B-27 Supplement	Th
Cellmatrix Type-IA (Collagen, Type !)	FU
Distilled Water	
DMEM-F12, CO2 independent (w/o Phenol red)	Sig
DMEM-F12, CO2 independent (with Phenol red)	Sig
HEPES-NAOH, pH 7.2, 1M (HEPES buffer)	Ca
L-Glutamine, 200 mM	Th
Mowiol 4-88	Sig
N-2 Supplement	Th
Neurobasal Medium	Th
Nuclease-free water	Th
O2 (40%), CO2 (5%), N2 (55%) Mix, 50 liters	
Paraformaldehyde	M
PBS	
Penicillin-Streptomycin (10,000 U/mL)	Th
Rat serum	Ch
	Ja
Sodium bicarbonate (NaHCO3)	M
Sodium hydroxide (NaOH)	M
Tyrode's salt	Sig

Equipment

Borosilicate glass capillaries, 1.2 mm outer diameter x 0.94 mm inner diameter | Su

Bottle-top filter system, 500 mL | Co
Computer PC
Custom pressure rig
Electronic pressure regulator | Pa

Falcon tubes, 15 mL | Co
Falcon tubes, 50 mL | Co
Fine-tip paintbrush
Flaming/ Brown micropipette puller | Su
Forceps, Dumont no. 3 | Fir
Forceps, Dumont no. 5 | Fir
Forceps, Dumont no. 55 | Fir
Heating block | Lal
Inverted fluorescence microscope | Ze
Light source | Ol
Manual pressure regulator | M

Microloader Tips | Ep
Microcontroller | Ar
Microscope camera Hamamatsu Orca Flash 4.0 V3
Motorized stage XY for microscope

rl Roth | Cat# 6351.2
ɜma-Aldrich | Cat# A2790
st Klebstoffe GmbH & Co.KG | Cat# CA221-10ml
ɪermo Fisher Scientific | Cat# 17504044
JJIFILM Wako Chemicals | Cat# 637-00653

ɜma-Aldrich | Cat# D2906
ɜma-Aldrich | Cat# D8900
rl Roth | Cat# 9105.3
ɪermo Fisher Sientific | Cat# 25030024
ɜma-Aldrich | Cat# 81381
ɪermo Fisher Scientific | Cat# 17502048
ɪermo Fisher Scientific | Cat# 21103049
ɪermo Fisher Scientific | Cat# AM9937

erck | Cat# 818715

ɪermo Fisher Scientific | Cat# 15140122
ɪarles River Laboratories
ɔan
erck | Cat# 106323
erck | Cat# 106482
ɜma | Cat# T2145-10x1L)

tter Instruments	Cat# BF-120-94-10
rning	Cat# 430769
rker Hannifin	Custom pressure rig Cat# 990-005101-002
rning	Cat# 430791
rning	Cat# 430829
tter Instruments	Cat# P-97
e Science Tools	Cat# 11231-30
e Science Tools	Cat# 11255-20
e Science Tools	Cat# 11252-20
btech International	Cat # Dri block Digi2
iss	Cat# Axiovert 200
ympus	Cat# Highlight 3100
cMaster Carr	Cat# 0-60 PSI 41795K3
pendorf	Cat# 5242956.003
duino	Cat# Arduino Due

Chemicals

Agarose, Low Melt

Agarose, Wild Range

Best-CA 221 Glue

B-27 Supplement

Cellmatrix Type-IA (Collagen, Type !)

Distilled Water

DMEM-F12, CO2 independent (w/o Phenol red)

DMEM-F12, CO2 independent (with Phenol red)

HEPES-NAOH, pH 7.2, 1M (HEPES buffer)

L-Glutamine, 200 mM

Mowiol 4-88

N-2 Supplement

Neurobasal Medium

Nuclease-free water

O2 (40%), CO2 (5%), N2 (55%) Mix, 50 liters

Paraformaldehyde

PBS

Penicillin-Streptomycin (10,000 U/mL)

Rat serum

Sodium bicarbonate (NaHCO3)

Sodium hydroxide (NaOH)

Tyrode's salt

Equipment

Borosilicate glass capillaries, 1.2 mm outer diameter x 0.94 mm inner diameter

Bottle-top filter system, 500 mL

Computer PC

Custom pressure rig

Electronic pressure regulator

Falcon tubes, 15 mL

Falcon tubes, 50 mL

Fine-tip paintbrush

Flaming/ Brown micropipette puller

Forceps, Dumont no. 3

Forceps, Dumont no. 5

Forceps, Dumont no. 55

Heating block

Inverted fluorescence microscope

Light source

Manual pressure regulator

Microloader Tips

Microcontroller

Microscope camera Hamamatsu Orca Flash 4.0 V3

Motorized stage XY for microscope

Multiwell plate, 24 wells

Pasteur pipettes, plastic

Petri dish, 60 x 15 mm

Petri dish, 35 x 10 mm

Petri dish, 34 x 14 mm, including Microwell no. 1.5 cover glass

Pipette holder

Pipette and tips

Puller filament, 3.0-mm square box filament

Slice culture incubation box

Solenoid valve

Stereomicroscope

Tabletop centrifuge

Thermometer

Three-axis Manipulator

Vibratome

Whole-embryo-culture-system incubator

Waterbath

Software and Algorithms

Arduino

Fiji

Python

ZEN

Carl Roth
Sigma-Aldrich
Best Klebstoffe GmbH & Co.KG
Thermo Fisher Scientific
FUJIFILM Wako Chemicals

Sigma-Aldrich
Sigma-Aldrich
Carl Roth
Thermo Fisher Sientific
Sigma-Aldrich
Thermo Fisher Scientific
Thermo Fisher Scientific
Thermo Fisher Scientific

Merck

Thermo Fisher Scientific
Charles River Laboratories
Japan
Merck
Merck

Sigma

Sutter Instruments

Corning

Parker Hannifin

Corning
Corning

Sutter Instruments
Fine Science Tools
Fine Science Tools
Fine Science Tools
Labtech International

Zeiss

Olympus

McMaster Carr

Eppendorf

Arduino

Nunc

Greiner

Nunc

MatTek

Warner Instruments

Sutter Instrument

MPI-CBG

Olympus

Heraeus

Sensapex Inc

Leica

Ikemoto Company

Arduino

Python Software foundation

Cat# 6351.2

Cat# A2790

Cat# CA221-10ml

Cat# 17504044

Cat# 637-00653

Cat# D2906

Cat# D8900

Cat# 9105.3

Cat# 25030024

Cat# 81381

Cat# 17502048

Cat# 21103049

Cat# AM9937

Cat# 818715

Cat# 15140122

Cat# 106323

Cat# 106482

Cat# T2145-10x1L)

Cat# BF-120-94-10

Cat# 430769

Custom pressure rig

Cat# 990-005101-002

Cat# 430791

Cat# 430829

Cat# P-97

Cat# 11231-30

Cat# 11255-20

Cat# 11252-20

Cat # Dri block Digi2

Cat# Axiovert 200

Cat# Highlight 3100

Cat# 0-60 PSI 41795K3

Cat# 5242956.003

Cat# Arduino Due

Cat# 142475

Cat# 628102

Cat# 153066

Cat# P35G-1.5-14-C

Cat# 64-2354 MP-s12u

Cat# FB330B

Cat# custom made

Cat# LHDA053321H-A

Cat# SZX12

Cat# 5431622

Cat# tree-axis uMP

Cat# VT1000s

Cat# RKI-10-0310

RRID: SCR_002285

Python 2.7.12

RRID: SCR_013672

Rebuttal letter
Shull at al.

1. The editor has formatted the manuscript to match the journal's style. Please retain and use the attached version.

We confirm we retained the formatting.

2. The manuscript needs thorough proofreading.

We proof read the manuscript.

3. Please ensure that the title of the manuscript is in line with the protocol presented.

We changed the title according to the Editor's request.

4. Please ensure that the result section is described in the context of the technique being presented.

We confirm the results section is described in the context of the technique being presented.

5. Please address all the specific comments marked in the manuscript.

We have addressed all the comments in the manuscript.

6. Once done please ensure that the protocol highlight is no more than 2.75 pages including headings and spacings.

We confirm that the protocol highlight is no more than 2.75 pages including headings and spacings.

7. Please move the troubleshooting to the discussion section in paragraph style. This can also be presented as a table in .xlsx format and referred to in the discussion section.

Following the Editor's suggestions, we created a separate file with the troubleshooting section.

8. Please reword Section 5 of the protocol as it matches with previously published literature.

We took care of rewording Section 5 according to the Editor's comment.

Troubleshooting

This section describes how to troubleshoot several common errors that arise when performing microinjection.

1) Error: The software reports an error message when loading in step 1.1.
    a) Causes:
        i)   The manipulator is not plugged into the computer via Ethernet.
        ii)   The manipulator is not turned on.
        iii) Two instances of the application are launched (two windows are open).
    b) Solution: Verify the manipulator is plugged into the computer and turn on the manipulator. Close the programs and wait two minutes to verify programs are shut. Relaunch the application.

2) Error: The video stream is not displayed in the software in step 1.1 and an error message says "CAMERA ERROR".
    a) Causes:
        i)   The camera is not turned on.
        ii)   The camera is not properly connected.
        iii) Two instances of the application are launched (two windows are open).
    b) Solution: Verify the camera is turned on and properly connected to the computer. Close all instances of the application.

3) Error: The pipette goes to first location but freezes in place when starting the microinjection in step 4.6.
    a) Causes: There is a connection problem with the microcontroller.
    b) Solution: Verify the microcontroller is plugged into the computer via USB. If the problem persists, plug the USB into a different USB port on the computer.

4) Error: The pipette is clogged.
    a) Causes:
        i)   Molecules in solution aggregated and clogged the tip.
        ii)   The pipette is not the ideal shape.
    b) Solution: Shake the injection solution and reload a different pipette. Pull the pipette at two degrees lower.

OPEN ACCESS

Authors of research articles can also opt to pay an article processing charge of $5,200 USD / £4,200 GBP / €4,700 EUR (+VAT where applicable) for their accepted articles to be open access online immediately upon publication. By paying this charge authors are also permitted to post the final, published PDF of their article on a website, institutional repository or other free public server, immediately on publication. If you cannot afford this fee, please contact the editorial office to discuss potential discounts. There are no additional page charges for Open Access papers.

EMBO Reports is included in the publishing agreement reached with 'Projekt DEAL', a consortium of universities and research institutes in Germany. Corresponding authors* affiliated with an eligible German institute or university may publish open access in *EMBO Reports* at no direct charge to the author with all OA-related costs being covered under the terms of the agreement (applies to all papers accepted after 30 June 2019). The default setting will be Open Access with a CC-BY license, but authors can choose another form of publication too.

Scientists based at eligible institutions in Germany now also receive free access to past and new content published in all the EMBO Press journals.

* You must be the submitting corresponding author and affiliated with a publicly or privately funded German research institution entitled under Projekt DEAL at the point of acceptance.